Huang, Wenmin; Han, Shijuan; Jiang, Hongsheng; Gu, Shuping; Li, Wei; Gontero, Brigitte; Maberly, Stephen C. 2020. **External α-carbonic anhydrase and solute carrier 4 are required for bicarbonate uptake in a freshwater angiosperm**.

# External α-carbonic anhydrase and solute carrier 4 (SLC4) are required for $HCO_3^-$ uptake in a freshwater angiosperm

Wenmin Huang[1,2], Shijuan Han[1,3], Hongsheng Jiang[1], Shuping Gu[4], Wei Li[1,*], Brigitte Gontero[2,*], Stephen C. Maberly[5,*]

[1] Key Laboratory of Aquatic Botany and Watershed Ecology, Wuhan Botanical Garden, Center of Plant Ecology, Core Botanical Gardens, Chinese Academy of Sciences, Wuhan 430074, China

[2] Aix Marseille Univ CNRS, BIP UMR 7281, IMM, FR 3479, 31 Chemin Joseph Aiguier, 13402 Marseille Cedex 20, France

[3] University of Chinese Academy of Sciences, Beijing 100049, China

[4] Shanghai Sequen Bio-info Studio, Shanghai, 200092, China

[5] Lake Ecosystems Group, UK Centre for Ecology & Hydrology, Lancaster Environment Centre, Library Avenue, Bailrigg, Lancaster LA1 4AP, UK

[*]Correspondence: Wei Li (liwei@wbgcas.cn), Brigitte Gontero (bmeunier@imm.cnrs.fr), Stephen C. Maberly (scm@ceh.ac.uk)

Highlight

Acquisition of $HCO_3^-$ in *Ottelia alismoides*, relies on co-diffusion of $CO_2$ and $HCO_3^-$ through the boundary-layer, conversion of $HCO_3^-$ to $CO_2$ at the plasmalemma by α-CA1 and transport by SLC4.

**Abstract**

The freshwater monocot *Ottelia alismoides* is the only known species to operate three $CO_2$ concentrating mechanisms (CCMs): constitutive $HCO_3^-$-use and C4 photosynthesis, and facultative Crassulacean acid metabolism, but the mechanism of $HCO_3^-$ use is unknown. We found that the inhibitor of an anion exchange (AE) protein, 4,4'-diisothio-cyanatostilbene-2,2'-disulfonate (DIDS), prevented $HCO_3^-$-use but also had a small effect on $CO_2$ uptake. An inhibitor of external carbonic anhydrase (CA), acetazolamide (AZ), reduced the affinity for $CO_2$ uptake but also prevented $HCO_3^-$ use via an effect on the AE protein. Analysis of mRNA transcripts identified a homologue of solute carrier 4 (SLC4) responsible for $HCO_3^-$ transport, likely to be the target of DIDS, and a periplasmic α-CA1. A model to quantify the contribution of the three different pathways involved in inorganic carbon uptake showed that passive $CO_2$ diffusion dominates inorganic carbon uptake at high $CO_2$ concentrations. However, as $CO_2$ concentrations fall, two other pathways become predominant: conversion of $HCO_3^-$ to $CO_2$ at the plasmalemma by α-CA1 and, transport of $HCO_3^-$ across the plasmalemma by SLC4. These mechanisms allow access to a much larger proportion of the inorganic carbon pool and continued photosynthesis during periods of strong carbon depletion in productive ecosystems.

**Keywords**

anion exchange protein, bicarbonate, carbonic anhydrase (CA), $CO_2$ concentrating mechanisms (CCMs), inorganic carbon acquisition, *Ottelia alismoides*, pH drift, photosynthesis, solute carrier 4 (SLC4)

## Introduction

Macrophytes form the base of the freshwater food web and are major contributors to primary production, especially in shallow systems (Silva *et al*., 2013; Maberly and Gontero, 2018). However, the supply of $CO_2$ for photosynthesis in water is potentially limited by the approximately 10,000 lower rate of diffusion compared to that in air (Raven, 1970). This imposes a large external transport resistance through the boundary layer (Black *et al*., 1981), that results in the $K_{½}$ for $CO_2$ uptake by macrophytes to be 100-200 μM, roughly 6-11 times air-equilibrium concentrations (Maberly and Madsen, 1998). Furthermore, in productive systems the concentration of $CO_2$ can be depleted close to zero (Maberly and Gontero, 2017). Freshwater plants have evolved diverse strategies to minimize inorganic carbon (Ci) limitation (Klavsen *et al*., 2011) including the active concentration of $CO_2$ at the active site of ribulose-1,5-bisphosphate carboxylase/oxygenase (Rubisco), collectively known as $CO_2$ concentrating mechanisms (CCMs). The most frequent CCM in freshwater plants is based on the biophysical uptake of bicarbonate ($HCO_3^-$), which is present in ~50% of the species tested (Maberly and Gontero, 2017; Iversen *et al*., 2019). While $CO_2$ can diffuse through the cell membrane passively, $HCO_3^-$ use requires active transport because the plasmalemma is impermeable to $HCO_3^-$ and the negative internal membrane potential (Denny and Weeks, 1970) produces a large electrochemical gradient resisting passive $HCO_3^-$ entry (Maberly and Gontero, 2018).

Detailed studies of the mechanisms of $HCO_3^-$ use have been carried out in microalgae, marine macroalgae, seagrasses and to a lesser extent, freshwater macrophytes (Giordano *et al*., 2005). Direct uptake/transport of $HCO_3^-$ can occur via an anion exchange protein (AE) located at the plasmalemma (Sharkia *et al*., 1994). Inhibition of this protein by the membrane impermeable and highly specific compound, 4,4'-diisothiocyanatostilbene-2,2'-disulfonate (DIDS), has confirmed its effect in a range of marine macroalgae and seagrasses (Drechsler *et al*., 1993; Björk *et al*., 1997; Fernández *et al*., 2014). Genomic studies have found that probable AE proteins, from the solute carrier 4 (SLC4) family bicarbonate transporters (Romero *et al*., 2013), also exist in marine microalgae (Nakajima *et al*., 2013; Poliner *et al*., 2015).

Carbonic anhydrase (CA) is a ubiquitous enzyme and is present in photosynthetic organisms. It interconverts $CO_2$ and $HCO_3^-$, maintaining equilibrium concentrations when rates of carbon transformation are high (Moroney *et al*., 2001; Dimario *et al*., 2018). External

carbonic anhydrase ($CA_{ext}$) is inhibited by the impermeable inhibitor acetazolamide (AZ). The widespread nature of $CA_{ext}$ is demonstrated by the inhibition of rates of photosynthesis in a range of aquatic photoautotrophs (James and Larkum, 1996; Larsson and Axelsson, 1999; Moroney *et al*., 2011; Tachibana *et al*., 2011; van Hille *et al*., 2014; Fernández *et al*., 2018). In many marine species, both $CA_{ext}$ and an AE protein are implicated in the uptake of $HCO_3^-$ but very little is known about freshwater macrophytes (Millhouse and Strother, 1986; Beer and Rehnberg, 1997; Björk *et al*., 1997; Gravot *et al*., 2010; Tsuji *et al*., 2017).

*Ottelia alismoides* (L.) Pers., a member of the monocot family Hydrocharitaceae, possesses two biochemical CCMs: constitutive C4 photosynthesis and facultative Crassulacean Acid Metabolism (CAM; Zhang *et al*., 2014; Shao *et al*., 2017; Huang *et al*., 2018). The leaves of *O. alismoides* comprise epidermal and mesophyll cells that contain chloroplasts and large air spaces but lack Kranz anatomy (Han *et al*., 2020). Although it is known that it can use $HCO_3^-$ in addition to $CO_2$, little is known about the mechanisms responsible for $HCO_3^-$ uptake. We have addressed this issue, with Ci uptake measurements using the pH-drift technique, experiments with inhibitors of CA and AE and analysis of transcriptomic data based on RNA analyzed from leaves acclimated at low and high $CO_2$ concentration. We hypothesize that external carbonic anhydrase and an AE protein will both be involved in $HCO_3^-$ uptake and that the contribution of these two mechanisms will alter as concentrations of $CO_2$ and $HCO_3^-$ change.

## Materials and methods

### *Plant material*

*O. alismoides* seeds were sown in soil from Donghu Lake, adjacent to the laboratory in Wuhan, that had been autoclaved to kill snail eggs and algae and covered with tap water, that had also been autoclaved, with an alkalinity of about 2.2 mequiv $L^{-1}$ and concentrations of Total Phosphorus and Total Nitrogen of about 0.05 and 1.35 mg $L^{-1}$ as described previously (Huang *et al*., 2018). After a month, seedlings were placed in three 400 L tanks (64 cm deep) receiving natural daylight in a glasshouse on the flat roof of the laboratory. The tap water in the tank was changed weekly and snails were removed daily. After nearly two months, the plants in the tanks had produced many mature leaves (see Supplementary Fig. S1).

*Experimental design and generation of low and high concentrations of $CO_2$*

There were three separate experiments. In one "pH-drift experiments", only a low-$CO_2$ treatment was used but in the two others ("Inhibitor experiments" and "Transcriptomic analyses") low- and high-$CO_2$ treatments were involved (Supplementary Fig. S1; Supplementary Table S1). In all the experiments, pH and temperature were measured every day with a combination pH electrode (E-201F, Shanghai Electronics Science Instrument Co., China) connected to a Thermo Orion Dual Star Benchtop pH/ISE Meter. The alkalinity was measured by Gran titration with a standard solution of HCl. $CO_2$ concentrations were calculated from pH, alkalinity, ionic strength and temperature using the equations in Maberly (1996).

Three series of experiment were performed. In the first experiment 'low $CO_2$', plants were grown in the large tanks in the glasshouse. Because of their high biomass, the plants generated high pH values (8.3-9.7) and low concentrations of $CO_2$ (0.1-6.2, mean 1.3 µM) in the tanks. Information of the conditions in the tanks is shown in Supplementary Table S1. In the second experiment 'low *vs* high $CO_2$', *O. alismoides* was incubated at high and low $CO_2$ concentration for 40 days in plastic containers within two of the tanks in the glasshouse as described previously (Zhang *et al*., 2014). The pH in the low $CO_2$ treatment (LC) ranged from 8.0 to over 9.8 and the $CO_2$ concentration ranged from 0.1 to 13 µM with a mean of 2.4 µM. For the high $CO_2$ treatment (HC), $CO_2$-saturated tap water was added to the buckets twice each day in order to keep the pH between 6.7-6.8, producing $CO_2$ concentrations between 481-1110 µM with a mean of 720 µM (Supplementary Table S1). pH-drifts were performed in the presence or absence of inhibitors AZ and DIDS on leaves from both experiments (see below) to determine their capacity to utilize $HCO_3^-$. In the third experiment, 'Transcriptomic analyses' changes in the transcription level of genes related to carbon acquisition were made on *O. alismoides* acclimated to LC and HC. *O. alismoides* plants were incubated in small containers in a growth room at 23.1-23.7 °C, 140-150 µmol photon $m^{-2}$ $s^{-1}$ and a 14 hour photoperiod as previously described (Huang *et al*., 2018). Low and high $CO_2$ were generated as described above; the concentration of $CO_2$ ranged between 0.1 and 5.1 µM with a mean of 1.1 µM in the LC treatment and between 301 and 604 µM with a mean of 307 µM in the HC treatment (Supplementary Table S1).

*pH-drift*

The pH-drift technique was used to determine the capacity of *O. alismoides* to utilize $HCO_3^-$, and the effects of inhibitors (AZ and DIDS) on photosynthetic Ci uptake. The method allows carbon uptake ability to be assessed by measuring pH over time and using it to calculate the concentration of the different inorganic carbon species as they become depleted by photosynthesis in a closed container (Maberly and Spence, 1983).. Prior to the start of the pH drift experiments, the leaves were collected from the glasshouse in the morning to avoid possible physiological differences caused by a light:dark rhythm of the plant, and then pieces of ~1.1 g fresh weight (FW) (roughly 0.1 g DW) of leaf tissue were cut and rinsed in the medium placed in a constant temperature room at 25 ± 2°C for around 1-4 hours before use. pH-drift experiments were made in a glass and plastic chamber (Maberly, 1990) containing 121 mL of 1 mM $HCO_3^-$ comprising equimolar concentration of $NaHCO_3$ and $KHCO_3$, a pH electrode (model IP-600-9 Jenco Instruments, USA) and an oxygen electrode (Unisense OX-13298). The chamber was placed in a water bath maintained at 25 ℃ and illuminated from the side by fluorescent tubes that provided 75 µmol photon $m^{-2}$ $s^{-1}$ (400-700 nm, Li-Cor sensor connected to a Li-Cor LI-1400 data logger) that was adequate to prevent light limitation at the low $CO_2$ concentrations studied in this experiment. The medium in the incubation chamber was initially bubbled with $N_2$ to reduce $O_2$ concentration ~100 ± 20 µM (about 40% air-equilibrium), which was detected by the oxygen electrode connected to an Unisense microsensor multimeter (Version 2.01) and recorded on a laptop computer. At the start of all drift experiments, the pH of the medium was set to 7.6 with $CO_2$-bubbled medium, and the subsequent changes were measured with the pH electrode connected to a pH meter (model 6311, Jenco Instruments, USA), and recorded on a monitor (TP-LINK, TL-IPC42A-4). The pH-drifts, undertaken at least in triplicate, with leaves from different tanks, took 6-23 h to reach an end point value (final pH), which was deemed to be achieved when the pH changed less than 0.01 unit in one hour (Maberly, 1990). After each drift, the dry weight of the plant material and the alkalinity of the medium were measured. The concentration of Ci was calculated as described above and Ci uptake rates calculated from changes in Ci concentration over time, chamber volume and plant mass (Maberly and Spence, 1983). When photosynthetic Ci uptake rates were plotted against the total carbon concentration ($C_T$) at which the rate occurred, a two-phased response curve was observed. The linear response at higher $C_T$ concentration was the consequence of $CO_2$ use, and the extrapolated intercept with

the $C_T$ axis corresponded to the $CO_2$ compensation point (Maberly and Spence, 1983). An example is shown in Supplementary Fig. S2.

*Inhibitor experiments*

For the inhibition experiments, a stock solution of AZ (20 mM) was prepared by dissolving the solid in 20 mM NaOH and 0.61 or 1.21 mL was injected into the chamber to produce final concentration of 0.1 or 0.2 mM respectively. Stock solutions of 30 mM DIDS, were prepared daily by dissolving the powder in distilled water (Cabantchik and Greger, 1992), and 1.21 mL was injected into the chamber to produce a final concentration of 0.3 mM. Both stock solutions were kept in the dark at 4°C.

To check if the inhibitory effect of AZ on $HCO_3^-$ uptake was reversible, we performed three consecutive drifts using the same *O. alismoides* leaf cut longitudinally into two halves. The first half was used as a control (first drift) without AZ. The second half was treated with AZ (second drift). Subsequently, this leaf and chamber were thoroughly rinsed with clean medium three times over ten minutes, and finally a post-control (third drift), was performed without the inhibitor. All the pH-drifts were started at pH 7.6 and stopped at pH 8.5 and replicated at least in triplicate.

$CA_{ext}$ activity was measured as in Fernández *et al*. (2018) with small modifications, using commercial CA (Sigma, C4396) as a positive control and to check activity linearity (Supplementary Fig. S3). A 50 mL plastic tube was placed inside a container filled with ice that maintained the temperature at 0-4°C. Approximately 60 mg FW leaf was placed in the tube containing 10 mL of buffer (pH 8.5): 50 mM Tris, 2 mM dithiothreitol, 15 mM ascorbic acid, 5 mM $Na_2$-EDTA and 0.3% w/v polyvinylpyrrolidone (PVP). Temperature and pH were simultaneously measured using a pH meter. The reaction was started by rapidly introducing 5 mL of ice-cold $CO_2$ saturated water and pH was recorded over time. The relative enzyme activity (REA) was determined using the equation below:

$$REA = (T_b/T_s)-1 \quad (1)$$

where $T_b$ and $T_s$ are the times in seconds required for the pH to drop from pH 8.3 to 7.9 in the non-catalyzed (without sample) and catalyzed reactions, respectively. The REA was

expressed on a fresh weight basis. In the leaves grown at LC and HC, external CA activity was measured in the presence of 0.1 mM and 0.2 mM AZ as well as 0.3 mM DIDS.

*Transcriptomic analyses*

Six samples (three HC and three LC acclimated mature leaves) were used for second-generation sequencing (SGS) for short but high-accuracy reads (Hackl *et al*., 2014). Six other samples were used for the third-generation sequencing (TGS) for longer sequences but lower-quality reads (Roberts *et al*., 2013). $CA_{ext}$ and AE proteins were searched for within the transcriptome dataset obtained from *O. alismoides* acclimated to LC and HC.

Around 0.3 g FW leaves were collected 30 minutes before the end of the photoperiod, flash frozen in liquid $N_2$ and stored at -80°C before use. Total RNA was extracted using a commercial kit RNAiso (Takara Biotechnology, Dalian, China). The purified RNA was dissolved in RNase-free water, with genomic DNA contamination removed using TURBO DNase I (Promega, Beijing, China). RNA quality was checked with the Agilent 2100 Bioanalyzer (Agilent Technologies, Palo Alto, California). Only the total RNA samples with RNA integrity numbers ≥8 were used to construct the cDNA libraries in PacBio or Illumina Hiseq sequencing.

For TGS analysis, total RNA (2 μg) was reversely transcribed into cDNA using the SMARTer PCR cDNA Synthesis Kit that has been optimized for preparing high-quality, full-length cDNAs (Takara Biotechnology, Dalian, China), followed by size fractionation using the BluePippin™ Size Selection System (Sage Science, Beverly, MA). Each SMRT bell library was constructed using 1-2 μg size-selected cDNA with the Pacific Biosciences DNA Template Prep Kit 2.0. SMRT sequencing was then performed on the Pacific Bioscience sequel platform using the manufacturer's protocol.

For SGS analysis, cDNA libraries were constructed using a NEBNext® Ultra™ RNA Library Prep Kit for Illumina® (NEB, Beverly, MA, USA), following the manufacturer's protocol. Qualified libraries were sequenced, and 150 bp paired-end reads were generated (Illumina Hiseq 2500, San Diego, CA, USA).

The TGS subreads were filtered using the standard protocols in the SMRT analysis software suite (http://www.pacificbiosciences.com) and reads of insert (ROIs) were

generated. Full-length non-chimeric reads (FLNC) and non-full-length cDNA reads (NFL) were recognized through the identification of poly(A) signal and 5' and 3' adaptors. The FLNC reads were clustered and polished by the Quiver program with the assistance of NFL reads, producing high-quality isoforms (HQ) and low-quality isoforms (LQ). The raw Illumina reads were filtered to remove ambiguous reads with 'N' bases, adaptor sequences and low-quality reads. Filtered Illumina data were then used to polish the LQ reads using the proovread 213.841 software. The redundant isoforms were then removed to generate a high-quality transcript dataset for *O. alismoides*, using the program CD-HIT.

TransDecoder v2.0.1 (https://transdecoder.github.io/ ) was used to define the putative coding sequence (CDS) of these transcripts. The predicted CDS were then functional annotated and confirmed by BLAST, which was conducted against the following databases: NR, NT, KOG, COG, KEGG, Swissprot and GO. For each transcript in each database searched, the functional information of the best matched sequence was assigned to the query transcript. The phylogenetic tree of α-CA1 and SLC4 isoforms based on deduced CA and $HCO_3^-$ transporters peptide sequences from the NCBI, was analyzed with Geneious software (Windows version 11.0, Biomatters Ltd, New Zealand). The location of the protein was analyzed using TargetP 1 (Emanuelsson *et al*., 2007; http://www.cbs.dtu.dk/services/TargetP/ ).

*Statistical analysis*

All data presented in this study are the mean ± SD. Mean final pH values were calculated geometrically because pH is on a log scale. One-way ANOVA was used to test for significant variation, after homogeneity and normality were satisfied. Duncan's and Tukey's post-hoc tests were used to test for significance among treatments while percentage data were compared using a non-parametric Mann–Whitney test. The threshold of statistical significance was set at $P<0.05$. The data were analyzed using SPSS 16.0 (SPSS Inc., Chicago, IL, USA).

**Results**

In control leaves, the pH drift end point was reached after nearly 24 hours at a mean pH of 10.2 (Fig. 1A, Supplementary Fig. S4) and a very low final $CO_2$ concentration of ~0.03 µM (about 0.2% of air-equilibrium) and at an oxygen concentration of about 353 µM (about 137% of air-equilibrium; Fig. 1B). This indicates that $HCO_3^-$ had been used, driving down the final $CO_2$ concentration, because the $CO_2$ compensation point of C3 and C4 plants would be about 40 and 5 times higher than this. In leaves treated with AZ or DIDS, the pH drift stopped after 6 to 12 hours and the end point did not exceed pH 9.3; final $CO_2$ concentrations were between 0.8 and 1.6 µM (Fig. 1A, 1B, Supplementary Fig. S4), indicating that $HCO_3^-$ use had been inhibited. As a consequence of $HCO_3^-$ use in control leaves, rates of Ci uptake were about 40 µmol $g^{-1}$ dry weight (DW) $h^{-1}$ even at the very low $CO_2$ concentrations (Supplementary Fig. S5). The slope of Ci uptake *vs* concentration of $CO_2$ between 15 and 40 µM in leaves treated with AZ was between 46% and 29% of the control ($P<0.05$) and in leaves treated with DIDS, it was about 65% of the control ($P<0.05$; Fig. 1C). In contrast, the intercept $CO_2$ compensation points increased significantly as a result of the addition of AZ (Fig. 1D). The higher AZ concentration treatments had a $CO_2$ compensation concentration close to 20 µM (at an oxygen concentration of 163 µM) suggesting that CCM is absent. These results suggest that AZ not only inhibited $CA_{ext}$ but also inhibited the AE protein. The $CO_2$ compensation concentration in the presence of DIDS, at about 5 µM (at an oxygen concentration of 232 µM, about 90% of air-equilibrium), was not significantly different from the control but substantially lower than in the two AZ treatments (Fig. 1D). The $C_T$/alkalinity quotient (the remaining total Ci at the end of the drift, $C_T$ related to the alkalinity) is a measure of the effectiveness of Ci depletion (Maberly and Spence, 1983). A low quotient indicates that a large proportion of the Ci pool is available for acquisition and vice versa. While $HCO_3^-$ use in control leaves allowed about half of the available inorganic carbon to be accessible, in the AZ and DIDS treated leaves, a high quotient was obtained and only between 11 and 16% of the available inorganic carbon was accessible (Fig. 1E).

Figure 2 shows the Ci uptake rates at different $CO_2$ concentrations calculated from the pH-drift experiments over a pH range from about 7.7 to 9.3. AZ inhibited Ci-uptake at all the $CO_2$ concentrations (Fig. 2A), and both AZ concentrations inhibited Ci uptake by between 70 and 76% when the concentrations of $CO_2$ were between 2.6 and 11 µM (Fig. 2B). In contrast, DIDS did not affect Ci uptake at $CO_2$ concentrations of 7 µM and above, but inhibited Ci uptake by about 40% at $CO_2$ concentrations between about 1 and 4 µM (Fig. 2B). The

inhibitory effect caused by AZ at both concentrations, can be completely reversed by washing since the post-control rates of Ci uptake were not significantly different from the initial control ($P>0.05$; Fig. 3). This confirms that AZ does not penetrate the plasmalemma (Moroney *et al*., 1985) and thus that the observed effects are linked to inhibition of $CA_{ext}$.

The inhibition of Ci uptake rates in the presence of 0.1 mM AZ and 0.3 mM DIDS were not significantly different in leaves acclimated to HC *vs* LC, although there was a slightly greater inhibition by 0.2 mM AZ in HC compared to LC leaves ($P<0.05$; Fig. 4A, 4B). $CA_{ext}$ activity was present in both HC and LC leaves but it was greater in LC leaves ($P<0.01$; Fig. 4C). $CA_{ext}$ activity was inhibited by AZ: the 0.2 mM treatment caused a greater inhibition than 0.1 mM AZ (Fig. 4D). DIDS had no effect on $CA_{ext}$ activity neither in HC nor in LC leaves. Moreover, the Ci uptake rates, from the control as well as the inhibitors-treated leaves at an initial $CO_2$ concentration of 12 µM (Fig. 4A), were broadly positively related to the activity of $CA_{ext}$ (Fig. 4C; $R^2 = 0.84$ and 0.74 for HC and LC leaves respectively, $P<0.01$).

The inhibition of Ci uptake in *O. alismoides* by AZ and DIDS implied that both $CA_{ext}$ and anion exchange protein were present. This was characterized further using transcriptomic analysis: mRNA for putative alpha carbonic anhydrase 1 (α-CA1) and $HCO_3^-$ transporters were expressed. Fifty-three transcripts were functionally annotated to CA according to sequence similarity and translated into 66 peptides. Six of these peptides were homologous with α-CA1, based on a comparison of amino acid sequences with the NCBI database, corresponding to four CA isoforms (Supplementary Fig. S6A, S7A). Isoform 1 in *O. alismoides* shows 60% and 61% identity with the chloroplastic isoform X1 and X2 of α-CA1 from the monocot *Musa acuminata*. Isoforms 2, 3 and 4 show 58%, 55% and 56% identity with the isoform X1 from this species, respectively, as well as 59%, 57% and 58% identity with the isoform X2. However, according to TargetP 1 software, all the isoforms from *O. alismoides* were predicted to be localized in the secretory pathway (Table 1). The expression of the four isoforms of putative α-CA1, was not significantly different in HC and LC acclimated leaves ($P>0.05$, Fig. 5A). Three other internally-located types of CA were detected (data not shown), but since they are not linked to the inhibition by AZ they were not analyzed further here.

Thirty-two peptides sequences from the SGS dataset were functionally annotated as a '$HCO_3^-$ transporter' or a 'boron transporter'. When these were analyzed using BLASTP, seven transcripts contained a Band 3 anion exchange domain, known to exist in anion

exchange protein 1 or SLC4 member 1 (Supplementary Fig. S6B) and corresponded to seven isoforms (Supplementary Fig. S7B). Of these, only one transcript, 27032, with 726 amino acid residues could be analyzed and TargetP 1 software predicted its location in the 'other' category that includes the plasmalemma (Table 1). Transcript 27032 had high identities with boron transporters that belong to the SLC4 family (Thurtle-Schmid and Stroud, 2016): for example, we found 84.8% identity in the monocot *Oryza sativa*, 80.0% identity in the dicot *Camellia sinensis*, 73.7% identity in the monocot seagrass *Zostera marina*, and 54.6% identity in the chlorophyte *Tetrabaena socialis*. Transcript 27032 also had high identities with $HCO_3^-$ transporters: for example, 79.4% in the dicot *Theobroma cacao*, 43.9% in the prasinophyte *Chloropicon primus*, 30.6% in the diatom *Fragilariopsis cylindrus* and 29.2% in the rhodophyte *Chondrus crispus*. Finally, transcript 27032 had high identities with uncharacterized proteins in diatoms: for example, 42.4% in *Thalassiosira oceanica*, 39.0% in *Thalassiosira pseudonana*, 36.3% in *Fistulifera solaria* and 29.6% in *Phaeodactylum tricornutum*. The mRNA expression of all the transcripts for putative SLC4 were not significantly different in HC and LC acclimated leaves of *O. alismoides* ($P>0.05$, Fig. 5B).

**Discussion**

*O. alismoides* possesses three CCMs, including constitutive abilities to (i) use $HCO_3^-$ and (ii) operate C4 photosynthesis, and (iii) a facultative ability to perform CAM when acclimated to low $CO_2$ concentrations (Zhang *et al*., 2014; Shao *et al*., 2017; Huang *et al*., 2018). This confirms our hypothesis that *O. alismoides* has a constitutive ability to use $HCO_3^-$, that relies on the action of an external carbonic anhydrase, α-CA1, and an anion exchange protein, SLC4 in the plasmalemma that together allows this species to exploit a large proportion of the Ci pool and drive $CO_2$ to very low concentrations.

In this study, multiple lines of evidence show that an external CA, putative α-CA1, plays a major role in Ci uptake in *O. alismoides*: (i) external CA activity was measured, (ii) AZ inhibited Ci uptake with the slope of Ci uptake *vs* the concentration of $CO_2$ between 15 and 40 µM being about a quarter of the control after treatment with 0.2 mM AZ, (iii) transcripts of putative α-CA1 were detected. The CA was confirmed to be external since (i) washing of leaves treated with AZ, restored CA activity and (ii) its sequence bears a signal peptide

consistent with a periplasmic location. External CA is indeed widespread in photoautotrophs from marine and freshwater environments (Moroney *et al*., 2001; Dimario *et al*., 2018). The green microalga *Chlamydomonas reinhardtii* has three α-CAs, of which two (Cah1 and Cah2) are localized in the periplasmic space and one (Cah3) in the thylakoid membrane (Fujiwara *et al*., 1990; Karlsson *et al*., 1998; Moroney and Chen, 1998). Eight classes of CA are currently known and although they all catalyze the same reaction, their primary amino acid sequence can be very different and as low as 7% (Jensen *et al*., 2019, 2020). The α-CA1 from *O. alismoides* has around 30% sequence identity with the periplasmic Cah1 from *C. reinhardtii*. The activity and transcript expression of many CAs are up-regulated at low concentrations of $CO_2$. The diatom *P. tricornutum* does not possess external CA, but the internal CA (β-type CA) is $CO_2$ responsive and crucial for its CCM operation (Satoh *et al*., 2001; Harada *et al*., 2005; Harada and Matsuda, 2005; Tsuji *et al*., 2017). In the marine diatom, *T. pseudonana*, the two external CAs, δ-CA and ζ-CA, as well as a recently identified chloroplastic ι-CA are induced by carbon limitation (Samukawa *et al*., 2014; Clement *et al*., 2017; Jensen *et al*., 2019). In contrast, the putative α-CA1 in *O. alismoides* is constitutive and its expression was unaffected by the $CO_2$ concentration that is consistent with $HCO_3^-$-use also being constitutive. This is also true for Cah3 in the thylakoid lumen of *C. reinhardtii* (Karlsson *et al*., 1998; Moroney and Chen, 1998). The expression of the periplasmic CA (Cah1) and the mitochondrial CAs (β-CA1 and β-CA2) are highly induced at low $CO_2$ (Moroney and Chen, 1998). However, in the case of Cah1, a knock-out mutant of *C. reinhardtii* had growth and photosynthesis characteristics that were similar to the wild type, suggesting it is not an essential component of the CCM (Van and Spalding, 1999).

We show that the anion exchange proteins, one group of the SLC4 family $HCO_3^-$ transporters (Romero *et al*., 2013), is involved in $HCO_3^-$ uptake in *O. alismoides*. DIDS, a commonly-used inhibitor of AE/SLC-type $HCO_3^-$ transporters (Romero *et al*., 2013) significantly decreased the final pH of a drift, and increased the final $CO_2$ concentration to about 0.8 µM which is not substantially less than that expected in the absence of a CCM: a terrestrial $C_3$ plant $CO_2$ compensation point of 36 µL $L^{-1}$ (Bauer and Martha, 1981) is equivalent to about 1.2 µM. Furthermore, transcripts of putative $HCO_3^-$ transporter family in *O. alismoides* were found to contain Band 3 anion exchange proteins (SLC4 member 1). More broad evidence from physiological data has demonstrated that anion exchange proteins play a role in $HCO_3^-$ uptake in green, red and brown marine macroalgae (Drechsler *et al*., 1993; Granbom and Pedersén, 1999; Larsson and Axelsson, 1999; Fernández *et al*., 2014).

Although $HCO_3^-$ use by seagrasses is known to involve an anion exchange protein, to our knowledge, this is the first report that provides evidence of the presence of direct $HCO_3^-$ uptake via DIDS-sensitive SLC4 $HCO_3^-$ transporters in an aquatic angiosperm.

Another strategy to use $HCO_3^-$ occurs in some species of freshwater macrophytes involving 'polar leaves' (Steemann-Nielsen, 1947). At the lower surface of these leaves, proton extrusion generates low pH that converts $HCO_3^-$ to $CO_2$ near the plasmalemma facilitating the passive uptake of Ci (Prins *et al*., 1980). It is unclear if *O. alismoides* has polar leaves as it does not produce dense marl layers on its upper surface. There is also some indirect evidence for a lack of polar leaves in *O. alismoides* since the limited data suggest that species with polar leaves, such as *Potamogeton lucens*, lack external CA (Staal *et al*., 1989) or in the case of *Elodea canadensis*, have CA activity that is not influenced by the $CO_2$ concentration (Elzenga and Prins, 1988) unlike *O. alismoides*.

It was initially surprising that AZ completely inhibited $HCO_3^-$ use. However, Sterling *et al*. (2001) also found that AZ inhibited AE1-mediated chloride-bicarbonate exchange. This result could be explained by the binding of CA to the AE resulting in the formation of a transport metabolon, where there was a direct transfer of $HCO_3^-$ from CA active site to the $HCO_3^-$ transporter (Sowah and Casey, 2011; Thornell and Bevensee, 2015). Thus, when CA is inhibited, then the transport of $HCO_3^-$ is inhibited. The putative SLC4 in *O. alismoides* has a C-terminus that is predicted to be exposed outside the plasma membrane using the TMHMM server v2 (Supplementary Fig. S8), in contrast to *P. tricornutum* with a SDDV sequence (Nakajima *et al*., 2013) orientated inside the cell. Since the internal C-terminus in *P. tricornutum* has been suggested to interact with internal CA, we hypothesize that the external SLC4 C-terminus could interact with external CA, but further work is required to test this and determine the residues involved.

*O. alismoides* can perform C4 photosynthesis, however the final $CO_2$ concentration at the end of pH-drift, when $HCO_3^-$-use was abolished by the inhibitors, was 0.8-1.6 µM, which could be supported by passive entry of $CO_2$ without the need to invoke a CCM. These are slightly higher than the $CO_2$ compensation point in the freshwater C4 macrophyte *Hydrilla verticillata* at less than 10 ppm (Bowes, 2010), which is equivalent to a dissolved $CO_2$ ~0.3 µM at 25 °C. If this difference between the species is real and not methodological, it could suggest that in *O. alismoides* C4 photosynthesis is more important to suppress photorespiration than to uptake carbon.

A simple model of carbon acquisition (Fig. 6A) was constructed to quantify the contribution of the three pathways involved in Ci uptake in *O. alismoides*: passive diffusion of $CO_2$, $HCO_3^-$-use involving α-CA1 and $HCO_3^-$-use involving SLC4 $HCO_3^-$ transporters. Using the Ci uptake rates at different $CO_2$ concentrations in Figure 2, and assuming that 0.3 mM DIDS completely inhibited $HCO_3^-$ transporters and that 0.2 mM AZ completely inhibited α-CA1 and $HCO_3^-$ transporters, we calculated: i) passive diffusion of $CO_2$ as the rate in the 0.2 mM AZ treatment that inhibited both α-CA1 and SLC4 $HCO_3^-$ transporters; ii) diffusion of $HCO_3^-$ and conversion to $CO_2$ by α-CA1 at the plasmalemma as the difference between the rate in the presence of 0.3 mM DIDS and that in the presence of 0.2 mM AZ; and iii) diffusion of $HCO_3^-$ and transfer across the plasmalemma by SLC4 $HCO_3^-$ transporters as the difference in the rate between the control and the 0.3 mM DIDS treatment. Unlike models for microalgae (e.g. Badger *et al*., 1994; Nakajima *et al*., 2013) where both the ratio of surface area to volume (Han *et al*., 2020), and the ratio of internal to external Ci concentration (Reiskind *et al*., 1997) are greater than in submerged macrophytes, we did not include Ci leakage in the model or distinguish between net and gross photosynthesis. At a $CO_2$ concentration of about 50 µM, passive diffusion of $CO_2$ contributed 55.7% to total Ci uptake, diffusion of $HCO_3^-$ and conversion to $CO_2$ by α-CA1 contributed 42.7% and transfer of $HCO_3^-$ across the plasmalemma by SLC4 $HCO_3^-$ transporters contributed 1.6% (Fig. 6B). At ~9 µM (about 66% of equilibrium with air at 400 ppm $CO_2$) the contribution to total Ci uptake of $CO_2$-diffusion, $HCO_3^-$ diffusion and conversion to $CO_2$ by α-CA1 and transfer by SLC4 $HCO_3^-$ transporters was 24.0%, 64.4% and 11.5% respectively and at about 1 µM $CO_2$ (close to a typical C3 $CO_2$ compensation point) diffusion was zero and α-CA1 and SLC4 $HCO_3^-$ transporters contributed equally to carbon uptake. So, as $CO_2$ concentrations fall, passive $CO_2$ diffusion can no longer support Ci uptake and indirect and direct use of $HCO_3^-$ allows Ci uptake to continue. The stimulation of absolute rates of SLC4 $HCO_3^-$ transporters-dependent Ci uptake is consistent with patterns seen for a number of freshwater macrophytes during pH-drift experiments, where rates increase as $CO_2$ approaches zero before declining as Ci is strongly depleted (Maberly and Spence, 1983). This could be caused by regulation or by direct effects of pH on $HCO_3^-$ transporter activity.

The model suggests that external CA is important in Ci uptake in *O. alismoides* and this is similar to results from seagrasses. External CA contributed 25% to Ci uptake in *Posidonia australis* (James and Larkum, 1996) and ~60% in *Zostera marina* (approximately 2.2 mM Ci at pH 8.2, equivalent to a dissolved $CO_2$ ~23 µM at 25 °C; Beer and Rehnberg, 1997), albeit

in the presence of Tricine buffer that might inhibit the photosynthesis rate. The contribution of external CA reported here for *O. alismoides* at a $CO_2$ concentration of 23 µM, 56%, is similar to that for *Z. marina*.

In conclusion, *O. alismoides* has developed a 'jack of all trades' CCM, the master of which, either external CA or SLC4 $HCO_3^-$ transporters, is the $CO_2$ concentration. There are several future lines of work that need to be pursued. The distribution of $HCO_3^-$ transporters in freshwater species should be determined. The apparent relationship between polar leaves and low or absent external CA activity could be tested using a range of species, especially within the genus *Ottelia* where calcite precipitation differs among species (Cao *et al*., 2019). The Ci acquisition mechanisms of more freshwater species should be examined. The cause of the increasing rate of $HCO_3^-$ transporters-dependent $HCO_3^-$ uptake as Ci becomes depleted needs to be understood. Finally, production and analysis of genome sequences for freshwater macrophytes will be a powerful tool to answer these and future questions concerning the strategies used by freshwater macrophytes to optimize photosynthesis.

## Data Availability

The data that support the findings of this study are available within the supplementary materials published online and from the first author (Wenmin Huang) on request.


## Acknowledgements

This work was supported by the Strategic Priority Research Program of the Chinese Academy of Sciences (Grant No. XDB31000000), Chinese Academy of Sciences President's International Fellowship Initiative to SCM and BG (2015VBA023, 2016VBA006), and the National Natural Science Foundation of China (Grant No. 31970368).


## Author contributions

All authors contributed to the design of the experiments, WH and SH performed the lab experiments, HJ and SG led the transcriptomic analyses, WH, HJ, BG and SCM analysed the data and led the drafting of the manuscript and all authors contributed and approved the final version.

## References


**Badger MR, Palmqvist K, Yu JW.** 1994. Measurement of $CO_2$ and $HCO_3^-$ fluxes in cyanobacteria and microalgae during steady-state photosynthesis. Physiologia Plantarum **90**, 529–536.

**Bauer H, Martha P.** 1981. The $CO_2$ compensation point of C3 plants-A re-examination I. Interspecific variability. Zeitschrift für Pflanzenphysiologie **103,** 445–450.

**Beer S, Rehnberg J.** 1997. The acquisition of inorganic carbon by the seagrass *Zostera marina*. Aquatic Botany **56,** 277–283.

**Björk M, Weil A, Semesi S, Beer S.** 1997. Photosynthetic utilization of inorganic carbon by seagrasses from Zanzibar, East Africa. Marine Biology **129,** 363–366.

**Black MA, Maberly SC, Spence DHN.** 1981. Resistance to carbon dioxide fixation in four submerged freshwater macrophytes. New Phytologist **89,** 557–568.

**Bowes G.** 2010. Chapter 5 Single-Cell C4 Photosynthesis in Aquatic Plants. In: Raghavendra A, Sage R. (eds) C4 Photosynthesis and Related $CO_2$ Concentrating Mechanisms. Advances in Photosynthesis and Respiration **32**, 63–80. Springer, Dordrecht.

**Cabantchik ZI, Greger R.** 1992. Chemical probes for anion transporters of mammalian cell membranes. American Journal of Physiology **262,** C803–C827.

**Cao Y, Liu Y, Ndirangu L, Li W, Xian L, Jiang HS.** 2019. The analysis of leaf traits of eight *Ottelia* populations and their potential ecosystem functions in Karst freshwaters in China. Frontiers in Plant Science **9,** 1938.

**Clement R, Lignon S, Mansuelle P, Jensen E, Pophillat M, Lebrun R, Denis Y, Puppo C, Maberly SC, Gontero B.** 2017. Responses of the marine diatom *Thalassiosira pseudonana* to changes in $CO_2$ concentration: a proteomic approach. Scientific Reports **7,** 42333.

**Denny P, Weeks DC.** 1970. Effects of light and bicarbonate on membrane potential in *Potamogeton schweinfurthii* (Benn). Annals of Botany **34,** 483–496.

**DiMario RJ, Machingura MC, Waldrop GL, Moroney JV.** 2018. The many types of carbonic anhydrases in photosynthetic organisms. Plant Science **268,** 11–17.

**Drechsler Z, Sharkia R, Cabantchik ZI, Beer S.** 1993. Bicarbonate uptake in the marine macroalga *Ulva* sp. is inhibited by classical probes of anion exchange by red blood cells. Planta **191,** 34–40.

**Elzenga JTM, Prins HBA.** 1988. Adaptation of *Elodea* and *Potamogeton* to different inorganic carbon levels and the mechanism for photosynthetic bicarbonate utilization. Australian Journal of Plant Physiology **15,** 727–735.

**Emanuelsson O, Brunak S, von Heijne G, Nielsen H.** 2007. Locating proteins in the cell using TargetP, SignalP and related tools. Nature Protocol **2,** 953–971.

**Fernández PA, Hurd CL, Roleda MY.** 2014. Bicarbonate uptake via an anion exchange protein is the main mechanism of inorganic carbon acquisition by the giant kelp *Macrocystis pyrifera* (Laminariales, Phaeophyceae) under variable pH. Journal of Phycology **50,** 998–1008.

**Fernández PA, Roleda MY, Rautenberger R, Hurd CL.** 2018. Carbonic anhydrase activity in seaweeds: overview and recommendations for measuring activity with an electrometric method, using *Macrocystis pyrifera* as a model species. Marine Biology **165,** 88.

**Fujiwara S, Fukuzawa H, Tachiki A, Miyachi S.** 1990. Structure and differential expression of 2 genes encoding carbonic-anhydrase in *Chlamydomonas reinhardtii*. Proceedings of the National Academy of Sciences USA **87,** 9779–9783.

**Giordano M, Beardall J, Raven JA.** 2005. $CO_2$ concentrating mechanisms in algae: mechanisms, environmental modulation, and evolution. Annual Review of Plant Biology **56,** 99–131.

**Granbom M, Pedersén M.** 1999. Carbon acquisition strategies of the red alga *Eucheuma denticulatum*. Hydrobiologia **398/399,** 349–354.

**Gravot A, Dittami SM, Rousvoal S, Lugan R, Eggert A, Collen J, Boyen C, Bouchereau A, Tonon T.** 2010. Diurnal oscillations of metabolite abundances

and gene analysis provide new insights into central metabolic processes of the brown alga *Ectocarpus siliculosus*. New Phytologist **188,** 98–110.

**Hackl T, Hedrich R, Schultz J, Förster F.** 2014. Proovread: large-scale high-accuracy pacbio correction through iterative short read consensus. Bioinformatics **30,** 3004–3011.

**Han SJ, Maberly SC, Gontero B, Xing ZF, Li W, Jiang HS, Huang WM.** 2020. Structural basis for $C_4$ photosynthesis without Kranz anatomy in leaves of the submerged freshwater plant *Ottelia alismoides.* Annals of Botany **125,** 869–879.

**Harada H, Matsuda Y.** 2005. Identification and characterization of a new carbonic anhydrase in the marine diatom *Phaeodactylum tricornutum*. Canadian Journal of Botany **83,** 909–916.

**Harada H, Nakatsuma D, Ishida M, Matsuda Y.** 2005. Regulation of the expression of intracellular β-carbonic anhydrase in response to $CO_2$ and light in the marine diatom *Phaeodactylum tricornutum*. Plant Physiology **139,** 1041–1050.

**Huang WM, Shao H, Zhou SN, Zhou Q, Fu WL, Zhang T, Jiang HS, Li W, Gontero B, Maberly SC.** 2018. Different $CO_2$ acclimation strategies in juvenile and mature leaves of *Ottelia alismoides*. Photosynthesis Research **138,** 219–232.

**Iversen LL, Winkel A, Baastrup-Spohr L, Hinke AB, Alahuhta J, Baatrup-Pedersen A, Birk S, Brodersen P, Chambers PA, Ecke F, Feldmann T, Gebler D, Heino J, Jespersen TS, Moe SJ, Riis T, Sass L, Vestergaard O, Maberly SC, Sand-Jensen K, Pedersen O.** 2019. Catchment properties and the photosynthetic trait composition of freshwater plant communities. Science **366,** 878–881.

**James PL, Larkum AWD.** 1996. Photosynthetic inorganic carbon acquisition of *Posidonia australis*. Aquatic Botany **55,** 149–157.

**Jensen EL, Clement R, Kosta A, Maberly SC, Gontero B.** 2019. A new widespread subclass of carbonic anhydrase in marine phytoplankton. The ISME Journal **13,** 2094–2106.

**Jensen EL, Maberly SC, Gontero B.** 2020. Insights on the functions and ecophysiological relevance of the diverse carbonic anhydrases in microalgae. International Journal of Molecular Sciences **21**, 2922.

**Karlsson J, Clarke AK, Chen ZY, Hugghins SY, Park YI, Husic HD, Moroney JV, Samuelsson G.** 1998. A novel alpha-type carbonic anhydrase associated with the thylakoid membrane in *Chlamydomonas reinhardtii* is required for growth at ambient $CO_2$. EMBO Journal **17,** 1208–1216.

**Klavsen SK, Madsen TV, Maberly SC.** 2011. Crassulacean acid metabolism in the context of other carbon-concentrating mechanisms in freshwater plants: a review. Photosynthesis Research **109,** 269–279.

**Larsson C, Axelsson L.** 1999. Bicarbonate uptake and utilization in marine macroalgae. European Journal of Phycology **34,** 79–86.

**Maberly SC, Spence DHN.** 1983. Photosynthetic inorganic carbon use by freshwater plants. Journal of Ecology **71,** 705–724.

**Maberly SC.** 1990. Exogenous sources of inorganic carbon for photosynthesis by marine macroalgae. Journal of Phycology **26,** 439–449.

**Maberly SC.** 1996. Diel, episodic and seasonal changes in pH and concentrations of inorganic carbon in a productive lake. Freshwater Biology **35,** 579–598.

**Maberly SC, Madsen TV.** 1998. Affinity for $CO_2$ in relation to the ability of freshwater macrophytes to use $HCO_3$. Functional Ecology **12,** 99–106.

**Maberly SC, Gontero B.** 2017. Ecological imperatives for aquatic $CO_2$-concentrating mechanisms. Journal of Experimental Botany **68,** 3797–3814.

**Maberly SC, Gontero B.** 2018. Trade-offs and synergies in the structural and functional characteristics of leaves photosynthesizing in aquatic environments. In: Adams III WW, Terashima I. (eds.) The leaf: a platform for performing photosynthesis. Advances in photosynthesis and respiration (Including bioenergy and related processes). Springer, Cham. 307–343.

**Millhouse J, Strother S.** 1986. Salt-stimulated bicarbonate-dependent photosynthesis in the marine angiosperm *Zostera muelleri*. Journal of Experimental Botany **37,** 965–976.

**Moroney JV, Husic HD, Tolbert NE.** 1985. Effect of carbonic anhydrase inhibitors on inorganic carbon accumulation by *Chlamydomonas reinhardtii*. Plant Physiology **79,** 177–183.

**Moroney JV, Chen ZY.** 1998. The role of the chloroplast in inorganic carbon uptake by eukaryotic algae. Canadian Journal of Botany **76,** 1025–1034.

**Moroney JV, Bartlett SG, Samuelsson G.** 2001. Carbonic anhydrases in plants and algae. Plant, Cell & Environment **24,** 141–153.

**Moroney JV, Ma Y, Frey WD, Fusilier KA, Pham TT, Simms TA, DiMario RJ, Yang J, Mukherjee B.** 2011. The carbonic anhydrase isoforms of *Chlamydomonas reinhardtii*: intracellular location, expression, and physiological roles. Photosynthesis Research **109,** 133–149.

**Nakajima K, Tanaka A, Matsuda Y.** 2013. SLC4 family transporters in a marine diatom directly pump bicarbonate from seawater. Proceedings of the National Academy of Sciences USA **110,** 1767–1772.

**Poliner E, Panchy N, Newton L, Wu G, Lapinsky A, Bullard B, Zienkiewicz A, Benning C, Shiu SH, Farré EM.** 2015. Transcriptional coordination of physiological responses in *Nannochloropsis oceanica* CCM1779 under light/dark cycles. Plant Journal **83,** 1097–1113.

**Prins HBA, Snel JFH, Helder RJ, Zanstra PE.** 1980. Photosynthetic $HCO_3^-$ utilization and $OH^-$ excretion in aquatic angiosperms: light induced pH changes at the leaf surface. Plant Physiology **66,** 818–822.

**Raven JA.** 1970. Exogenous inorganic carbon sources in plant photosynthesis. Biological Reviews **45,** 167–221.

**Reiskind JB, Madsen TV, Van Ginkel LC, Bowes G.** 1997. Evidence that inducible $C_4$-type photosynthesis is a chloroplastic $CO_2$-concentrating mechanism in *Hydrilla*, a submersed monocot. Plant, Cell & Environment **20**, 211–220.

**Roberts RJ, Carneiro MO, Schatz MC.** 2013. The advantages of SMRT sequencing. Genome Biology **14,** 405.

**Romero MF, Chen AP, Parker MD, Boron WF.** 2013. The SLC4 family of bicarbonate ($HCO_3^-$) transporters. Molecular Aspects of Medicine **34,** 159–182.

**Samukawa M, Shen C, Hopkinson BM, Matsuda Y.** 2014. Localization of putative carbonic anhydrases in the marine diatom, *Thalassiosira pseudonana*. Photosynthsis Research **121,** 235–249.

**Satoh D, Hiraoka Y, Colman B, Matsuda Y.** 2001. Physiological and molecular biological characterization of intracellular carbonic anhydrase from the marine diatom *Phaeodactylum tricornutum.* Plant Physiology **126,** 1459–1470.

**Shao H, Gontero B, Maberly SC, Jiang HS, Cao Y, Li W, Huang WM.** 2017. Responses of *Ottelia alismoides*, an aquatic plant with three CCMs, to variable $CO_2$ and light. Journal of Experimental Botany **68,** 3985–3995.

**Sharkia R, Beer S, Cabantchik ZI.** 1994. A membrane-located polypeptide of *Ulva* sp. which may be involved in $HCO_3^-$ uptake is recognized by antibodies raised against the human red-blood-cell anion-exchange protein. Planta **194,** 247–249.

**Silva TSF, Melack JM, Novo EMLM.** 2013. Responses of aquatic macrophyte cover and productivity to flooding variability on the Amazon floodplain. Global Change Biology **19,** 3379–3389.

**Sowah D, Casey JR.** 2011. An intramolecular transport metabolon: fusion of carbonic anhydrase II to the COOH terminus of the $Cl^-/HCO_3^-$ exchanger, AE1. American Journal of Physiology-Cell Physiology **301,** C336–C346.

**Staal M, Elzenga JTM, Prins HBA.** 1989. $^{14}C$ fixation by leaves and leaf cell protoplasts of the submerged aquatic angiosperm *Potamogeton lucens:* carbon dioxide or bicarbonate? Plant Physiology **90,** 1035–1040.

**Steemann-Nielsen E.** 1947. Photosynthesis of aquatic plants with special reference to the carbon sources. Dansk Botanisk Arkiv Udgivet af Dansk Botanisk Forening **8,** 3–71.

**Sterling D, Reithmeier RAF, Casey JR.** 2001. A transport metabolon: Functional interaction of carbonic anhydrase II and chloride/bicarbonate exchangers. The Journal of Biological Chemistry **276,** 47886–47894.

**Tachibana M, Allen AE, Kikutani S, Endo Y, Bowler C, Matsuda Y.** 2011. Localization of putative carbonic anhydrases in two marine diatoms, *Phaeodactylum tricornutum* and *Thalassiosira pseudonana*. Photosynthesis Research **109,** 205–221.

**Thornell IM, Bevensee MO.** 2015. Regulators of *Slc4* bicarbonate transporter activity. Frontiers in Physiology **6,** 166.

**Thurtle-Schmidt BH, Stroud RM.** 2016. Structure of Bor1 supports an elevator transport mechanism for SLC4 anion exchangers. Proceedings of the National Academy of Sciences **113**, 10542–10546.

**Tsuji Y, Nakajima K, Matsuda Y.** 2017. Molecular aspects of the biophysical $CO_2$-concentrating mechanism and its regulation in marine diatoms. Journal of Experimental Botany **68,** 3763–3772.

**Van K, Spalding MH.** 1999. Periplasmic carbonic anhydrase structural gene (*Cah1*) mutant in *Chlamydomonas reinhardtii*. Plant Physiology **120**, 757–764.

**van Hille R, Fagan M, Bromfield L, Pott R.** 2014. A modified pH drift assay for inorganic carbon accumulation and external carbonic anhydrase activity in microalgae. Journal of Applied Phycology **26,** 377–385.

**Zhang YZ, Yin LY, Jiang HS, Li W, Gontero B, Maberly SC.** 2014. Biochemical and biophysical $CO_2$ concentrating mechanisms in two species of freshwater macrophyte within the genus *Ottelia* (Hydrocharitaceae). Photosynthesis Research **121,** 285–297.

**Table 1.** Predicted location of isoforms of α-CA1 and SLC4 in *O. alismoides*.

| Putative protein | Isoform | Transcript | Length | cTP | mTP | SP | Other | Loc | RC |
|---|---|---|---|---|---|---|---|---|---|
| α-CA1 | 1 | 25043 | 273 | 0.077 | 0.025 | 0.885 | 0.013 | SP | 1 |
| α-CA1 | 2 | 21823, 32613* | 266, 235 | 0.023 | 0.023 | 0.951 | 0.050 | SP | 1 |
| α-CA1 | 3 | 27301, 31599** | 266, 266 | 0.021 | 0.025 | 0.952 | 0.054 | SP | 1 |
| α-CA1 | 4 | 14247 | 234 | 0.023 | 0.023 | 0.951 | 0.050 | SP | 1 |
| SLC4*** | 1 | 27032 | 726 | 0.021 | 0.110 | 0.108 | 0.957 | Other | 1 |

Output from the TargetP 1 server using default settings. cTP, chloroplast transit peptide; mTP, mitochondrial targeting peptide; SP, secretory pathway; Other, other locations; Loc, final prediction; RC, reliability class (from 1 to 5), where 1 indicates the strongest prediction. *Transcript lacks a transit peptide at the N-terminus so it was not long enough to be analyzed; **Two identical transcripts; ***Isoform 1 of SLC4 was the only SLC4 transcript long enough to be analyzed.

**Figure legends**

**Fig. 1.** Analysis of pH drift experiments without (control) or with inhibitors (AZ and DIDS) in *O. alismoides*. (A) Final pH; (B) Final $CO_2$ concentration; (C) Initial slope of Ci uptake rate *vs* concentration of $CO_2$ (between 15~40 μM), $\alpha_C$; (D) $CO_2$ compensation point ($CP(CO_2)$); (E) $C_T$/Alk. Values represent means ± SD, n=3. Letters indicate statistical differences between control and treatments (one-way ANOVA, Duncan's and Tukey's post-hoc tests $P<0.05$).

**Fig. 2.** Effect of AZ or DIDS on the Ci uptake rate at different $CO_2$ concentrations in *O. alismoides*. (A) Ci uptake rate; (B) Ci uptake inhibition. Values represent means ± SD, n=3. Letters in (A) indicate statistical differences among control and inhibitor treatments within $CO_2$ concentrations (one-way ANOVA, Duncan's and Tukey's post-hoc tests $P<0.05$). Letters and symbols in (B) indicate statistical differences among different $CO_2$ concentrations within inhibitor treatment (Mann–Whitney test $P<0.05$).

**Fig. 3.** Effect of removal of AZ on Ci uptake rate in *O. alismoides* leaves at different $CO_2$ concentrations. Values represent means ± SD, n=3. (A) 0.1 mM AZ; (B) 0.2 mM AZ. The inhibitor was removed by washing the treated leaves in the post-control (see Methods). Letters indicate statistical differences between the control and inhibitor treatments of AZ for each $CO_2$ concentration (one-way ANOVA, Duncan's and Tukey's post-hoc tests $P<0.05$).

**Fig. 4.** Effect of AZ and DIDS on Ci uptake rate and external CA activity in leaves of *O. alismoides* acclimated to high $CO_2$ (HC) or low $CO_2$ (LC) and measured at an

initial $CO_2$ concentration of 12 μM. (A) Ci uptake rate; (B) Inhibition of Ci uptake rate; (C) External CA activity and (D) Inhibition of external CA activity. Values represent means ± SD, n=3. For panels (A) and (C), letters indicate statistical differences between the control and different treatments at HC and LC acclimated leaves using one-way ANOVA, Duncan's and Tukey's post-hoc tests $P<0.05$. For panels (B) and (D), uppercase and lowercase letters indicate statistical differences among inhibitor treatments at HC and LC respectively using the Mann–Whitney test $P<0.05$; the line above the two columns indicates the statistical differences between HC and LC treatments (Mann–Whitney test, $P<0.05$; NS not significant).

**Fig. 5.** Expression of mRNA encoding proteins implicated in carbon uptake in leaves of *O. alismoides* acclimated to high $CO_2$ (HC) or low $CO_2$ (LC). (A) α-CA1 isoforms; (B) SLC4 isoforms. Values represent the mean ± SD, n=3. The lines above the two columns indicate the statistical differences between LC and HC treatment (one-way ANOVA, $P<0.05$; NS not significant).

**Fig. 6.** A model of inorganic carbon acquisition in *O. alismoides*. (A) Model structure. ① passive diffusion of $CO_2$; ② diffusion of $HCO_3^-$ and conversion to $CO_2$ by α-CA1 at the plasmalemma; ③ diffusion of $HCO_3^-$ and transfer across the plasmalemma by SLC4 $HCO_3^-$ transporters. (B) The contribution of $CO_2$-diffusion, diffusion of $HCO_3^-$ and conversion to $CO_2$ via α-CA1 and transfer of $HCO_3^-$ by SLC4 $HCO_3^-$ transporters to total Ci uptake at different $CO_2$ concentrations.

Figure 1

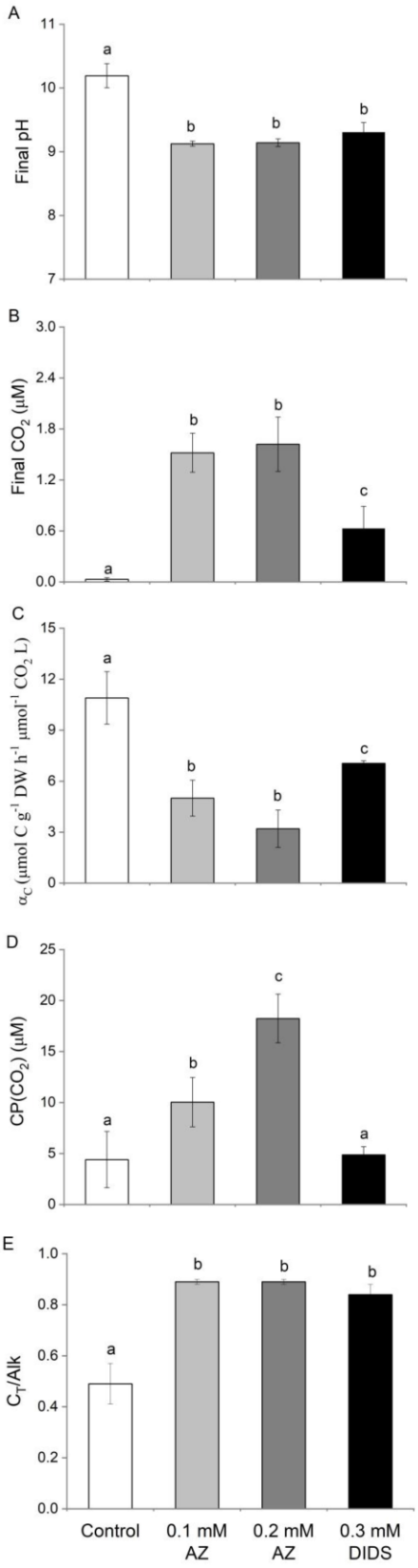

Figure 2

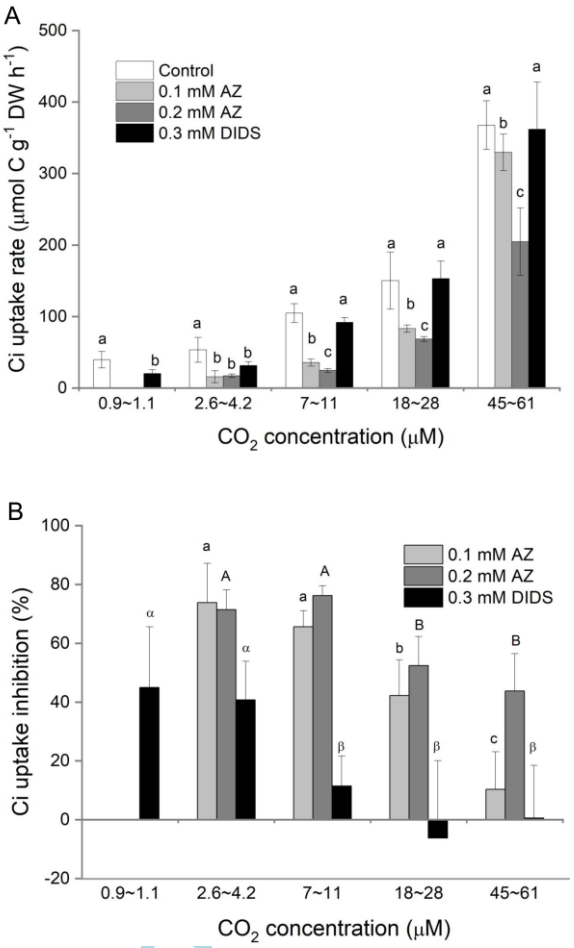

Figure 3

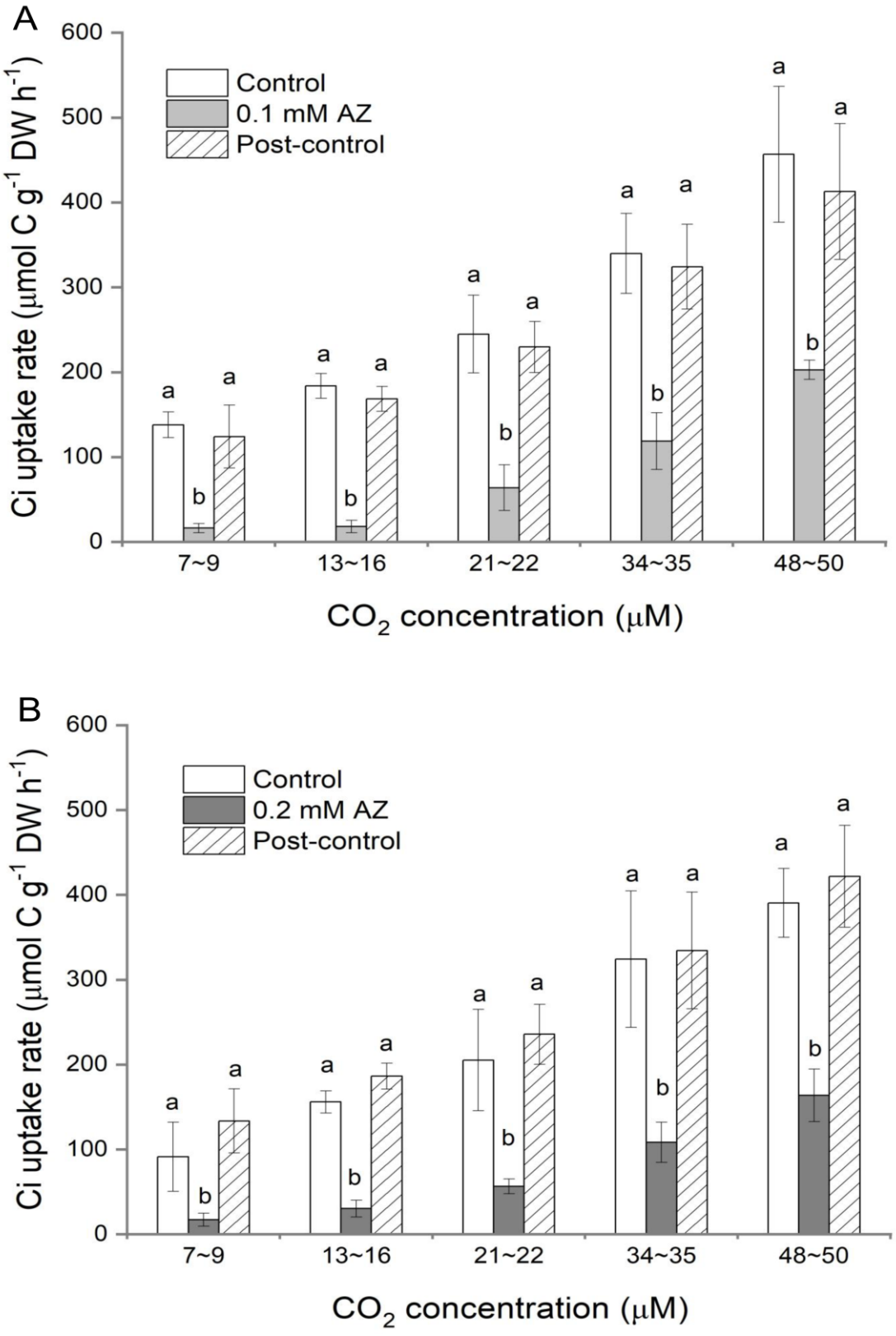
A
Ci uptake rate (μmol C g-1 DW h-1)
600
500
400
300
200
100
0
Control
0.1 mM AZ
Post-control
a
b
a
a
b
a
a
b
a
a
b
a
a
b
a
7~9
13~16
21~22
34~35
48~50
CO2 concentration (μM)
B
Ci uptake rate (μmol C g-1 DW h-1)
600
500
400
300
200
100
0
Control
0.2 mM AZ
Post-control
a
b
a
a
b
a
a
b
a
a
b
a
a
b
a
7~9
13~16
21~22
34~35
48~50
CO2 concentration (μM)

Figure 4

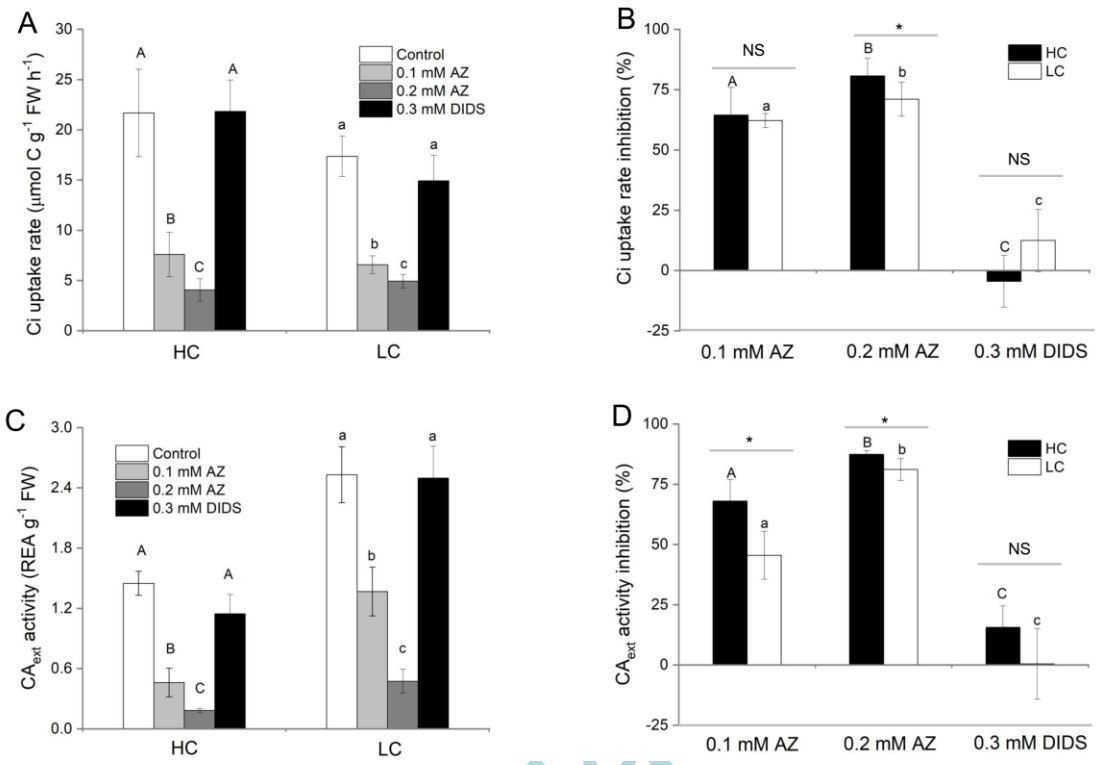

Figure 5

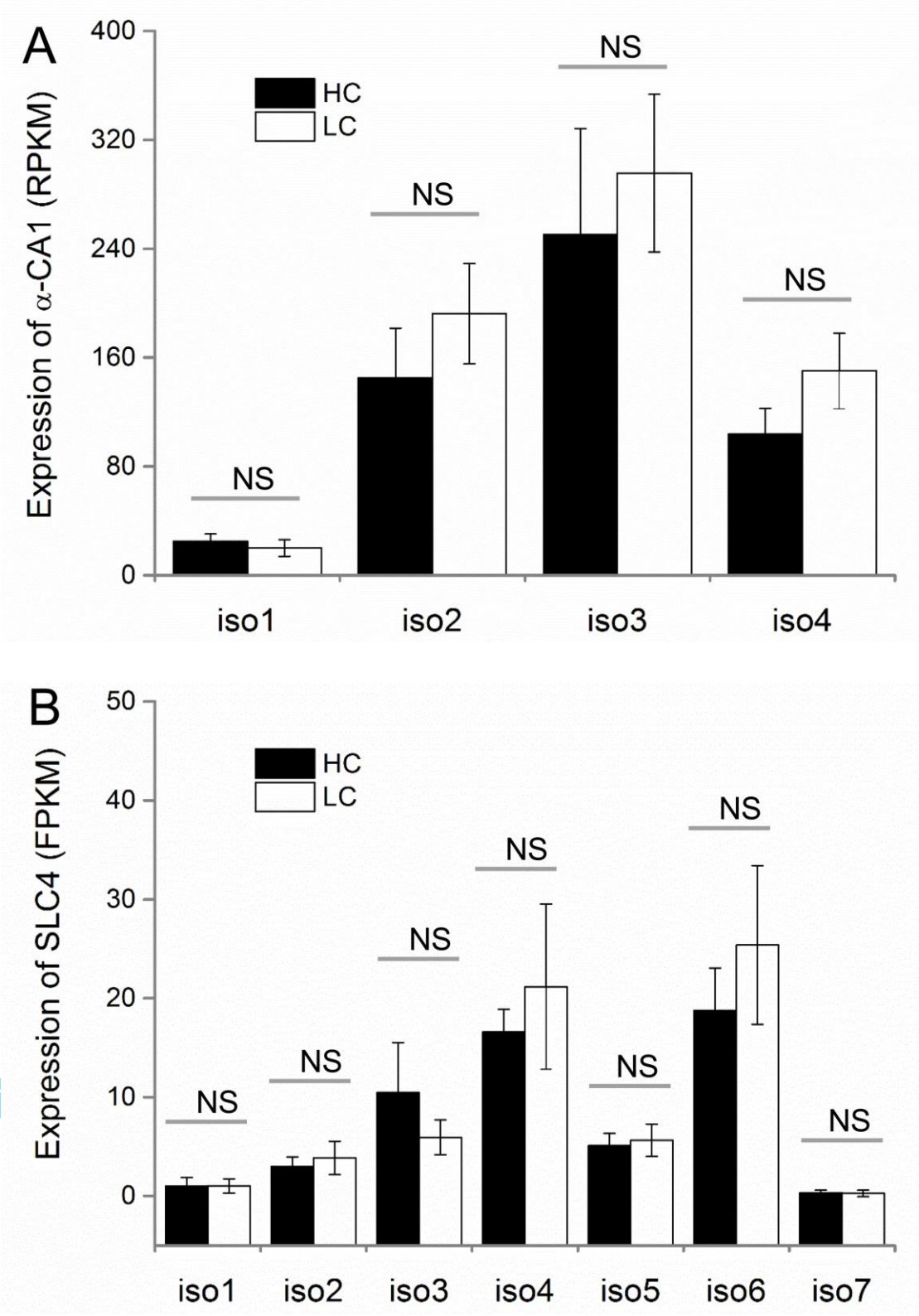
A
Expression of α-CA1 (RPKM)
400
320
240
160
80
0
HC
LC
NS
NS
NS
NS
iso1
iso2
iso3
iso4
B
Expression of SLC4 (FPKM)
50
40
30
20
10
0
HC
LC
NS
NS
NS
NS
NS
NS
iso1
iso2
iso3
iso4
iso5
iso6
iso7

Figure 6

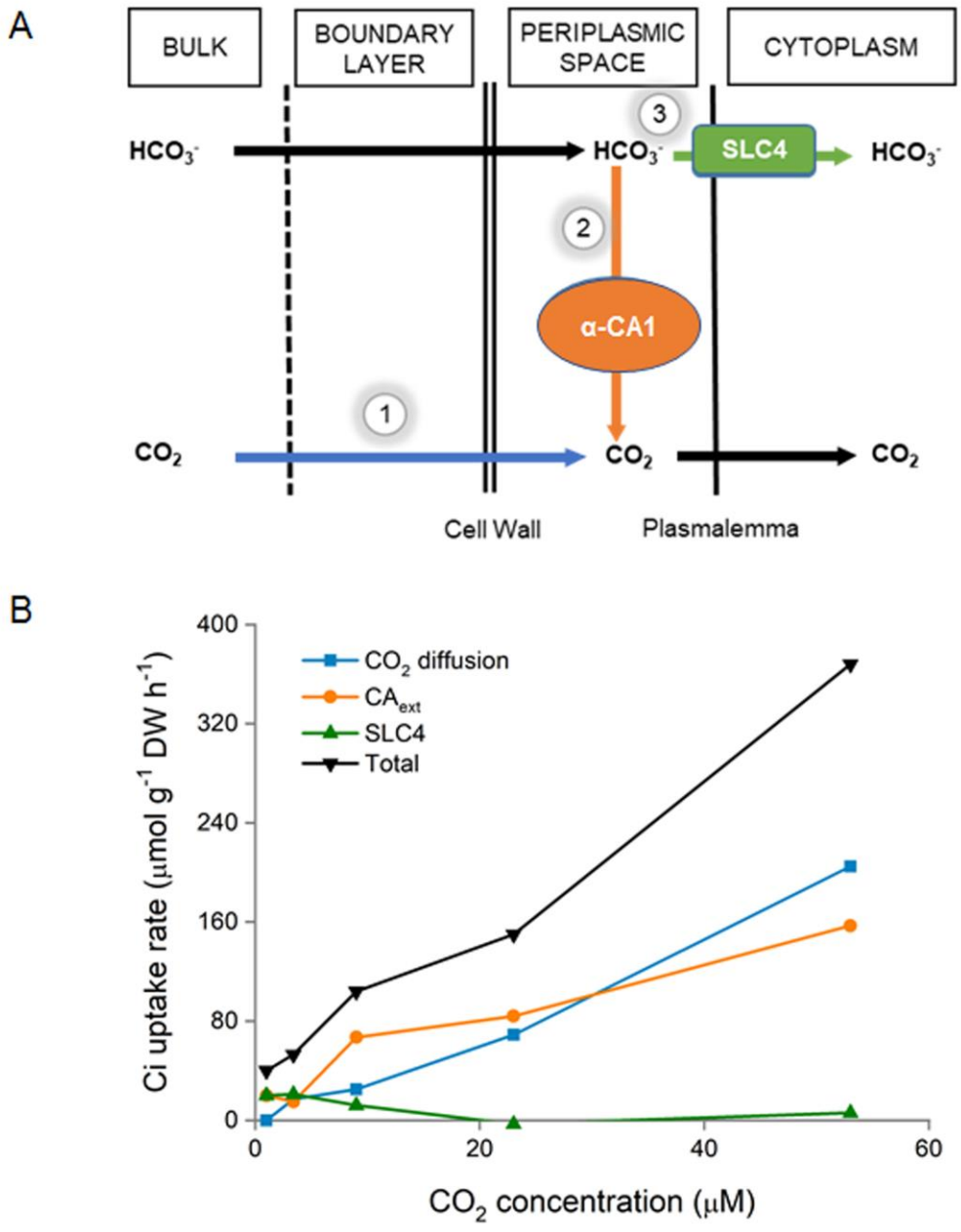
A
BULK
BOUNDARY LAYER
PERIPLASMIC SPACE
CYTOPLASM
HCO3-
HCO3-
SLC4
HCO3-
3
2
α-CA1
1
CO2
CO2
CO2
Cell Wall
Plasmalemma
B
Ci uptake rate (μmol g-1 DW h-1)
CO2 diffusion
CAext
SLC4
Total
400
320
240
160
80
0
0
20
40
60
CO2 concentration (μM)